Interference from alkene in chemiluminescent NOx measurements

Mohammed S. Alam[1], Leigh R. Crilley[1#], James D. Lee[2], Louisa J. Kramer[1], Christian Pfrang[1], Mónica Vázquez-Moreno[3*], Amalia Muñoz[3], Milagros Ródenas[3] and William J. Bloss[1]

[1]School of Geography, Earth and Environmental Sciences, University of Birmingham, Birmingham, B15 2TT, UK
[2]National Centre for Atmospheric Science, Wolfson Atmospheric Chemistry Laboratories, University of York, York, UK
[3]EUPHORE, Fundación CEAM, Valencia, Spain

now at: Department of Chemistry, York University, Toronto, ON, Canada
* now at: FISABIO, Valencia, Spain

Correspondence to: Mohammed S. Alam (m.s.alam@bham.ac.uk)

Abstract. Nitrogen oxides (NO_x = NO + NO_2) are critical intermediates in atmospheric chemistry and air pollution. NO_x levels control the cycling and hence abundance of the primary atmospheric oxidants OH and NO_3, and regulate the ozone production which results from the degradation of volatile organic compounds (VOCs) in the presence of sunlight. They are also atmospheric pollutants, and NO_2 is commonly included in air quality objectives and regulations. NO_x levels also affect the production of the nitrate component of secondary aerosol particles and other pollutants such as the lachrymator peroxyacetyl nitrate (PAN). The accurate measurement of NO and NO_2 is therefore crucial to air quality monitoring and understanding atmospheric composition. The most commonly used approach for measurement of NO is chemiluminescent detection of electronically excited NO_2 (NO_2^*), formed from the NO + O_3 reaction within the NO_x analyser. Alkenes, ubiquitous in the atmosphere from biogenic and anthropogenic sources, also react with ozone to produce chemiluminescence and thus may contribute to the measured NO_x signal. Their ozonolysis reaction may also be sufficiently rapid that their abundance in conventional instrument background cycles, which also utilises reaction with ozone, differs from that in the measurement cycle – such that the background subtraction is incomplete, and an interference effect results. This interference has been noted previously, and indeed the effect has been used to measure both alkenes and ozone in the atmosphere. Here we report the results of a systematic investigation of the response of a selection of commercial NO_x monitors, ranging from systems used for routine air quality monitoring to atmospheric research instrumentation, to a series of alkenes. The species investigated range from short chain alkenes, such as ethene, to the biogenic monoterpenes. Experiments were performed in the European Photoreactor (EUPHORE) to ensure common calibration and samples for the monitors, and to unequivocally confirm the alkene levels present (via FTIR). The instrument interference responses ranged from negligible levels up to 11 % depending upon the alkene present and conditions used (*e.g.* presence of co-reactants and differing humidity). Such interferences may be of substantial importance for the interpretation of ambient NO_x data, particularly for high-VOC, low-NO_x environments such as forests, or indoor environments where alkene abundance from personal care and cleaning products may be significant.

Introduction

Measurement of atmospheric trace constituents is central to atmospheric chemistry research and air pollution monitoring. Key challenges to trace measurements are sensitivity, reactivity and selectivity – as many components of interest are only present at ppb (parts per billion, 10^{-9}) or ppt (parts per trillion, 10^{-12}) mixing ratios; in many cases their inherent reactivity necessitates *in situ* detection, and because atmospheric trace composition comprises many thousands of different chemical components (Goldstein and Galbally, 2007). Consequently, specific measurement approaches have been developed to measure key atmospheric species, within the specific conditions (analyte abundance, presence of other constituents) anticipated (Heard, 2008). This paper reports a systematic study of the interference arising in measurements of the nitrogen oxides from the presence of alkenes in sampled air, when using their most widespread air quality monitoring technique of chemiluminescence detection.

NO_x (= NO + NO_2) abundance controls the cycling and hence concentration of the primary atmospheric oxidants, hydroxyl (OH) and nitrate (NO_3) radicals, and regulates the ozone production which results from the degradation of volatile organic compounds (VOCs) in sunlight. NO_x are also atmospheric pollutants in their own right, and NO_2 is commonly included in air quality objectives and regulations (as the more harmful component of NO_x) (European Environment Agency, 2018; Chaloulakou et al. (2008). In addition to their role in controlling ozone formation, NO_x levels affect the production of other pollutants such as the lachrymator peroxyacetyl nitrate (PAN), and the nitrate component of secondary aerosol particles. Consequently, accurate measurement of nitrogen oxides in the atmosphere is of major importance for monitoring pollution levels and assessing consequent health impacts, and understanding atmospheric chemical processing. Atmospheric NO and NO_2 are formed from natural processes (lightning, soil emissions of NO, biomass burning and even snowpack emissions) and anthropogenic activities (high temperature combustion in air leading to the breakdown of N_2 and O_2, and NO_x production via the Zeldovitch mechanism), where road traffic is the predominant source in many urban areas (Keuken *et al.*, 2009; Grice *et al.*, 2009; Carslaw and Rhys-Tyler, 2013). Consequently, boundary layer NO_x abundance varies over many orders of magnitude – from sub 5-ppt levels in the remote marine boundary layer, to ppm levels in some urban environments (Crawford *et al.*, 1997).

Techniques used for the measurement of atmospheric NO_x include laser-induced fluorescence spectroscopy (LIF), for both NO and NO_2; absorption spectroscopy (long-path and cavity-enhanced differential optical absorption spectroscopy, LP- and CE-DOAS, cavity attenuated phase shift spectroscopy (CAPS), cavity ring-down spectroscopy (CRDS), and passive diffusion tubes, primarily for NO_2), chemical ionisation mass spectrometry (CIMS) and both on- and offline wet chemical methods *e.g.* long path absorption photometer (LOPAP) (Heard, 2008; Sandholm et al. 1990; Kasyutich et al. 2003; Kebabian et al. 2005; Cape, 2009; Fuchs et al. 2009; Thalman and Volkamer, 2010; Villena et al. 2011). However, the most commonly employed

technique for the measurement of NO_x species, including for statutory air quality monitoring purposes, is the detection of the chemiluminescence arising from electronically excited NO_2 (NO_2^*) formed from the reaction between NO and O_3 (via R1):

$$NO + O_3 \rightarrow NO_2^* + O_2 \quad (R1)$$

$$NO_2^* \rightarrow NO_2 + h\nu \quad (R2)$$

The intensity of the light emitted via (R2) is in the wavelength 600 – 3000 nm, peaking at ~1200 nm. Chemiluminescent instruments mix sampled ambient air with a reagent stream containing an excess of ozone, to promote the chemiluminescent reaction (see schematic – Figure 1); the resulting emission signal is measured using a photomultiplier tube (PMT), and consists of contributions from NO_2^* formed as above, but also potentially from other chemiluminescence processes, detector dark counts and other noise contributions. Contributions to the measured emission from other species are minimised by using a red filter on the detector to block emission wavelengths below ca. 600 nm, and by employing a background subtraction cycle: chemiluminescent NO_x monitors commonly acquire a background by increasing the reaction time between NO (from the sampled air) and O_3 (reagent formed within the instrument), using a pre-reactor volume, such that nearly all of the NO present (specifications typically state, in excess of 99%) is converted to NO_2. The difference in PMT signals between the "online" and "background" signals is then taken to be proportional to the NO present in the air sample, following the assumption that the abundance of other species which may contribute to the measured signal is not affected by the background cycle.

Chemiluminescent instruments typically alternate between two operation modes – one that directly measures NO and one that measures $\Sigma(NO + NO_2)$, by first converting NO_2 to NO. The difference between the two values determines the NO_2 mixing ratio (if only NO and NO_2 are present). This is most commonly achieved using a molybdenum (Mo) catalyst heated to 300 – 350°C. However, the reduction of other NO_z species to NO have led to the use of these catalysts in chemiluminescent NO_y monitors to measure total reactive nitrogen rather than NO_2 ($NO_y = NO_z + NO_x$; and NO_z = other reactive nitrogen species catalysed by Mo convertors *e.g.* HNO_3, HONO, N_2O_5, HO_2NO_2, PAN, NO_3, organic nitrates – but not NH_3) (Navas *et al.*, 1997; Murphy *et al.*, 2007). If atmospheric mixing ratios of NO_z species are high relative to NO_2 then NO_2 measurements with monitors equipped with Mo catalysts are increasingly inaccurate. This has led to the adoption of photolytic NO_2 conversion stages in research instruments, where a blue light LED convertor is illuminated in a photolysis cell converting NO_2 to NO (Lee *et al.*, 2015).

$$NO_2 + h\nu\ (<420\ nm) \rightarrow NO + O(^3P) \quad (R3)$$

The photolytic conversion technique can have greater specificity than the heated Mo catalyst as the photolysis wavelengths may be selected to match the NO_2 photolysis action spectrum, while potential NO_z interferents for an NO_2 measurement are

thermally unstable and may convert to NO_2 when exposed to heat in the latter approach (Heard, 2008). Despite this, the chemiluminescent analyser with the heated Mo catalyst is the most widely used technique for air quality monitoring of NO and NO_2 worldwide. It is the reference method of measurement specified in the EU directive (BS EN 14211, 2012), providing real-time data with short time resolution for 212 monitoring sites in the UK, including kerbside, roadside, urban background, industrial and rural locations (Air Quality Expert Group, 2004).

Origins of interferences in chemiluminescent NO_x measurements

While NO_x measurements are sometimes perceived to be straightforward and routine, in practice a number of factors are known to affect the accuracy of the levels obtained using chemiluminescence approaches. A detailed account of factors affecting atmospheric NO_x measurement overall is given elsewhere (*e.g.* Gerboles *et al*., 2003; Villena *et al*., 2012; Reed *et al.*, 2016); here we do not focus upon surface sources/losses but rather upon chemical interferences in chemiluminescent NO_x analysers, which may arise from the following possible general mechanisms:

1. Collisional quenching of NO_2* by an interferent species with a greater collisional efficiency than the bath gas (e.g. air) used for calibration (typically a negative interference, although the magnitude and sign of this depends upon the calibration conditions employed)
2. Conversion of other N-containing species to NO_x within the NO_2 conversion unit (positive interference)
3. Chemical removal or interconversion of NO and/or NO_2 by an interferent species generated within the instrument (positive or negative interference)
4. Chemiluminescence of other chemical species, which is not fully accounted for during the instrument background cycle (positive interference)

Collisional quenching of excited species, mechanism (1), results in a reduction in the chemiluminescence intensity, to an extent dependent upon the pressure, and quenching efficiency – the efficacy with which the quenching species may accept or remove energy from the excited moiety. In the case of electronically excited NO_2, effective quenching agents have been shown to include H_2O, CO_2, H_2 and hydrocarbons (Matthews *et al*., 1977; Gerboles *et al*., 2003; Dillon and Crowley, 2018), of which only quenching by water vapour is considered to be significant under most common (ambient air) conditions – sensitivity reductions of up to 8 % have been reported (Steinbacher *et al*., 2007). Mechanism (2), conversion of other nitrogen-containing species to NO, alongside NO_2, is a recognised issue with heated Mo converters – interferences between 18 – 100 % have been reported for species such as HONO, HNO_3, PAN, alkyl nitrates and N_2O_5 (Dunlea *et al*., 2007; Lamsal *et al*., 2008). To address these uncertainties, photolytic converters are now commonly employed in research measurements, although for most routine air quality monitoring, heated Mo converters are still employed. Recently, it has been shown that a further interference can arise within the photolytic converter stage – from the generation of HO_x radicals through photolysis of photolabile carbonyl species such as glyoxal, forming peroxy radicals promoting NO-to-NO_2 conversion within the instrument (Villena *et al*., 2012),

resulting in a negative NO_2 interference, which may (under some conditions) exceed the positive interference from retrieval of NO_z species associated with heated Mo converter instruments i.e. mechanism (3).

The focus of this work relates to mechanism (4): interference in chemiluminescent measurements of NO and NO_2 (using both catalytic and photolytical converters) arising from the chemiluminescence of alkenes in the presence of ozone. Alkene-ozone reactions have received substantial attention as a dark source of HO_x radicals, and a route to the formation of semi-volatile compounds which contribute to secondary organic aerosol (SOA), particularly for biogenic alkenes such as isoprene and the mono- and sesquiterpenes (*e.g.* Johnson & Marston, 2008; Shrivastava *et al.*, 2017). Rate constants for ozonolysis reactions depend on alkene structure, and are typically larger for biogenic alkenes. Chemiluminescence from the ozonolysis of 14 short chain species at total pressures of 2 – 10 Torr was first reported by Pitts *et al*. (1972). Excited HCHO, vibrationally excited OH and electronically excited OH in the wavelengths 350 – 520 nm, 700 – 1100 nm and 306 nm, respectively, were the identified chemiluminescent species (Finlayson *et al.* (1974); and indeed has been used to perform field measurements of both ozone and alkenes (e.g. Velasco *et al.*, 2007; Hills and Zimmerman, 1990). This combination – of alkene-ozone reactions giving rise to a chemiluminescent interference signal, and alkene-ozone reactions being sufficiently rapid that alkenes can be appreciably consumed in the background (pre-reactor) cycle, and hence the interference contribution not fully subtracted during the background correction – gives rise to the potential for interference in NO_x measurements, which is the focus of this study.

Experimental Approach

Experiments were performed using chamber A of the two $200m^3$ simulation chambers of the European Photoreactor (EUPHORE) facility in Valencia, Spain to provide a common, homogeneous air volume for multiple NO_x analysers to sample from. The EUPHORE chambers are formed from fluorine-ethene-propene (FEP) Teflon foil fitted with housings that exclude ambient light (Wiesen, 2001; Munoz *et al.*, 2011). The chambers are fitted with large horizontal and vertical fans to ensure rapid mixing (timescale 3 minutes). Instrumentation used comprised long-path FTIR (for absolute and specific alkene / VOC measurements), monitors for temperature, pressure, humidity (dew-point hygrometer), ozone (UV absorption) and CO (infrared absorption). NO_x levels were measured using four independent chemiluminescent monitors, plus (in the case of NO_2) LP-DOAS absorption spectroscopy – All monitor sampling lines were similar lengths and attached to one inlet sampling from the centre of the chamber.

Monitors 1 and 2 employed heated Mo catalysts, while 3 and 4 used photolytic NO_2 converters (see Table 1). All NO_x monitors were calibrated (in the range 0 – 100 ppb) at the start and end of the two-week measurement period using a multi-point calibration derived from a primary NO standard (BOC 5 ppm alpha standard, certified to the NPL scale) in addition to single-point calibrations performed on a daily basis. NO_2 calibration was achieved via gas-phase titration using added ozone within

the chamber. In some experiments the calibrations and interference were confirmed with use of the EUPHORE long-path DOAS system to unequivocally identify and quantify NO_2.

All experiments were performed with the chamber housing closed (i.e. dark conditions, $j(NO_2) < 2\times10^{-6}$ s^{-1}), at near atmospheric pressure and ambient temperature. For most experiments, humidity was low (dew point ca. -45 ° C). The experimental procedure, starting with a clean flushed chamber, was to add SF_6 (as a dilution tracer), followed by successive aliquots of various alkenes and in certain cases additional species (H_2O and CO), whilst recording the measured NO and NO_2 levels, over periods of 1-3 hours. For some systems, ozone was added at the end of the experiment – under such dark, high O_3 conditions we can be confident that negligible NO could actually be present in the chamber (e.g. from wall sources) and hence that any "NO" signal observed by the monitors was unequivocally an interference response (as any NO remaining would be rapidly consumed by reaction with O_3). The potential interferant species investigated were cis-2-butene (C2B), trans-2-butene (T2B), tetra-methyl ethylene (2,3-dimethyl-butene or TME), α-terpinene, limonene, methyl chavicol (estragole) and terpinolene, with 4 – 5 additions of 20 – 50 ppb in each case, together with single- or dual-point interference measurements for ethene, propene, isobutene, isoprene, α-pinene, β-pinene and myrcene. Repeat experiments were performed for trans-2-butene, terpinolene and α-terpinene under conditions of increased humidity (up to ca. 30% RH). Alkene mixing ratios introduced into the chamber are given in Table S1. Propene, cis-2-butene and trans-2-butene where supplied by The Linde Group (purity > 99%); isobutene (purity > 99%) and terpinolene (purity > 85%) from Fluka Analytical; and TME (purity > 98%), isoprene (purity > 99%), limonene (purity > 97%), α-pinene (purity > 97%), β-pinene (purity > 97%), α-terpinene (purity > 85%), estragole (purity > 98%) and myrcene (purity > 99%) from Sigma Aldrich. All reagents were used as supplied.

Data Analysis

The limit of detection (LOD) for each instrument was determined under the actual experimental conditions, as three times the standard deviation of the NO and NO_2 signal recorded each day from the empty chamber prior to the start of experiments (*i.e.* before addition of any reactants). The mean LODs determined for NO and NO_2 are shown in Table 1. These LOD values are higher than those quoted by the manufacturers for monitors 1-4 (typically 2-100 ppt) but accurately reflect the actual performance of the instruments as used during these experiments. In the analysis which follows, in order to confirm that any change in measured NO and NO_2 mixing ratio for each alkene addition was not due to noise or drift and therefore signal, the readings were compared to the experimentally determined LOD for each instrument. Only if the measured change was greater than the experimentally determined LOD were these readings used for determining an interference. The interference due to the VOC was determined by means of linear regression (least squares fit), with slopes and their uncertainty and Pearson's correlation coefficients calculated in IGOR (see Tables 2 and 3).

Results

Figures 2-4 give the measured VOC mixing ratios and the retrieved "NO" and "NO_2" measurements by the four monitors during the experiment for selected alkenes, along with the regression analysis for determining the interference levels. Spikes in NO and NO_2 mixing ratios observed after an alkene addition (*e.g.* Fig. 4) arise from sampling close to the addition point prior to the initial period of mixing in the chamber (~ 3 min) and were disregarded in the analysis. The slow decay of alkene and "NO_x" mixing ratios following each addition arises from dilution effects (with a first order rate constant of ~ 5.7×10^{-5} s^{-1}, derived from the decay of SF_6).

From Figures 2-4, a clear and systematic response from the monitors to the presence of α-terpinene, terpinolene and trans-2-butene was observed, with the magnitude varying between the monitors. In addition to the alkenes shown in Figures 2-4, significant interference effects were also observed for cis-2-butene, TME and limonene for some of the monitors, as summarised in Tables 2 and 3. No interference was observed, within detection uncertainty, for ethene, propene, isobutene, α-pinene, β-pinene, myrcene or methyl chavicol in any of the monitors. For isoprene, no statistically significant interference was observed for monitors 1-3, while monitor 4 observed a very small positive interference of 0.035 ± 0.001% (NO channel) and 0.076 ± 0.002% (NO_2 channel).

For the alkenes where significant interference was observed, in general a positive interference was observed for NO and a negative interference for NO_2 by monitors 1-4 (Tables 2 and 3), with the exception of TME, where a negative NO interference was observed by monitor 3 (and is discussed later). Generally, for monitor 4 a positive NO interference, and a mixture of both positive and negative NO_2 interferences, was observed. Overall, while the magnitude of interference differed between the monitors, the same trend in the interference was observed, with α-terpinene having the largest interference effect, followed by terpinolene, TME/trans-2-butene, cis-2-butene and limonene.

The addition of water (RH ca. 30%) led to the observed NO and NO_2 interference for trans-2-butene, terpinolene and α-terpinene decreasing by 30 – 60% as shown in Tables 2 and 3. The addition of CO resulted in an increase in the NO interference observed for TME from below the LOD to 0.7% for monitors 1 and 2 while monitors 3 and 4 exhibited a larger interference increase (Table 2).

Discussion

Interference effects on retrieved NO abundance

Positive NO interferences were observed for those alkenes which react most rapidly with ozone, and hence will be present within the monitor reaction chamber at different levels in the measurement and background modes. This interference is

attributed to chemiluminescent emission following the alkene-ozone reaction, and may be attributed to a combination of two factors: formation of excited products in the alkene-ozone reaction which emit chemiluminescence, coupled with the significant removal of some alkenes during the instrument background phase compared with the measurement phase, through their reaction with (elevated levels of) ozone within the instrument, *i.e.* mechanism (4) outlined above.

Possible origins of this signal are the production of excited HCHO, vibrationally excited OH and electronically excited OH (*e.g.* Finlayson *et al.*, 1974). While the long-pass filters used in chemiluminescence NO_x monitors should preclude emission from electronically excited species, vibrationally excited OH produced through the hydroperoxide mechanism is known to emit in the 700 – 1100 nm wavelength range (Finlayson *et al.*, 1974; Schurath *et al.*, 1976; Hansen *et al.*, 1977; Toby, 1984), and would be detected as NO_2. The long-pass filters used in the chemiluminescence NO_x monitors in this study are not reported in their respective user manuals, but typically block light below ca. 600 nm, while typical PMT response characteristics are between 400 – 950 nm (Jernigan, 2001). Any chemiluminescence signal in the 600 – 950 nm wavelength range can therefore cause a potential interference.

The difference in the interference effect among monitors may then reflect differences in the conditions (*e.g.* ozone abundance, pressure, residence time) within the reaction cell and filter specifications. The relative magnitudes of the positive interference signals observed between the different monitors are consistent with this picture, as the reaction chamber pressure is much lower for monitors 3 and 4 (*ca.* 1 – 10 Torr) compared with monitors 1 and 2 (*ca.* 300 Torr) leading to greater collisional quenching. Similarly, addition of H_2O, which would be expected to efficiently accept vibrational energy from OH radicals (Gerboles *et al.*, 2003), was found to substantially reduce the apparent interference. In the experiments with higher humidity, a reduced interference (factor of *ca.* 2, see Table 2) was observed for all NO experiments for all instruments except for TME for the photolytic converters, where an increase was observed. There is currently no recommended relative humidity under which calibrations should be performed for any of the instruments or within EU and EPA guidelines (AQEG, 2004; USEPA, 2002). However, the installation of permeation driers at the sample inlet should (in principle) reduce the impact of different H_2O / relative humidity levels upon quenching of NO_2 or other species and are a common feature of most modern samplers (AQEG, 2004).

Interference magnitude: kinetic and structural effects

The most significant effects are the large positive NO interferences observed for the monoterpenes; α-terpinene and terpinolene, within monitors 1, 3 and 4. The criteria for an alkene to display such a positive interference (*i.e.* via mechanism 4) are that it reacts with ozone to produce suitable excited products which exhibit a chemiluminescent signal at appropriate wavelengths. In addition, the alkene must have a sufficiently rapid reaction with ozone that its mixing ratio is substantially reduced during the instrument background phase compared with the measurement phase, precluding the correct subtraction of

the interference signal. The reaction rate constants for many alkenes with ozone are well known, allowing the calculation of a kinetic interference potential (KIP) ranking for this second factor, and is calculated by Eq 1.

$$KIP = 100 \times \left(1 - exp^{(-k't \times \frac{k_{(Alkene+O_3)}}{k_{(NO+O_3)}})}\right) \quad \text{(Eq. 1)}$$

where $k' = k[O_3]t$ and $\frac{[NO]}{[NO]_0} = 0.01$ (*i.e.* 1% of NO left after reaction with excess O_3); see Supplementary Information for calculation details. The calculated KIP are shown in Table 4 as the percentage of a given alkene's potential chemiluminescent signal which would *not* be subtracted in the standard background cycle, under the assumption that the background cycle conditions (O_3 mixing ratio, residence time) would be sufficient to remove 99% of NO present.

This ranking does not reflect the precise (relative) interference which is observed, as it neglects structural features which will affect the yield (and state *i.e.* electronic or vibrationally excited) of the chemiluminescent products from the ozonolysis reaction – but is consistent with the trend and relative magnitudes for the substantial positive interferences shown in Tables 2 and 3. For example, a lack of interference is observed for myrcene and limonene, both of which exhibit terminal C=C bonds (see Table 4), and after reaction with ozone lead to the production of the CH_2OO Criegee intermediate (CI) which subsequently decomposes or undergoes rearrangement to form small yields of OH (Alam *et al*., 2011). The ozonolysis of internal alkenes such as cis- and trans-2-butene produce the CH_3CHOO CI which predominantly decomposes via the vinyl hydroperoxide mechanism forming larger yields of OH (Johnson and Marston, 2008; Alam *et al*., 2013). Such chemically formed OH that produces a detectable signal may also be augmented by contributions from HO_2 and RO_2, converted into OH within the instrument by reaction with NO – especially in the NO_2 channel of photolytic converter instruments.

The relationship between the KIP (Table 4) and measured NO interference (Tables 2 and 3) is illustrated in Figure 5 and can be used for predicting the potential interference of a given alkene to the NO signal form a kinetic perspective. For example, α-humulene has a KIP of 94.54% which could give rise to a 1.7%, 2.4% or 10.2% NO interference for monitors 1, 3 and 4, respectively. This estimate is, however, based on the rate constant of α-humulene alone and does not include any structural features such as the presence of terminal and non-terminal C=C bonds.

Explanation of the interference observed for NO_2

The above discussion considers only the interference effect arising from alkene chemiluminescent emission; further measurement impacts are also evident in the (negative) interferences apparent for other species / monitors in Tables 2 and 3.

Inspection of Tables 2 and 3 shows smaller positive interferences, and some negative interferences, from alkenes in the NO_2 measurements.

NO_2 measurements using chemiluminescence approaches are usually obtained by measuring NO_x (*i.e.* $\Sigma(NO + NO_2)$, after passing the sampled air through an NO_2 converter) and subtracting the (independently determined) NO contribution. If the actual interference signal (additional chemiluminescence) during the NO_x measurement mode arises solely from mechanism (4), ozonolysis chemiluminescence, then this would be expected to match that in the NO mode (subject to the alkene abundance not being altered in the NO_2 conversion stage and if the detection conditions for the NO and NO_x phases are identical), and consequently would not affect the retrieved NO_2 mixing ratio. Monitors 1, 2 and 3 used a single detection cell, alternating between NO and NO_2 (NO_x) modes, and so measured the NO_2* chemiluminescence signal under identical conditions (optical arrangement, filtering, pressure). The observed negative interference for NO_2 therefore may have arisen due to removal of alkene by the Mo catalyst within the monitors.

For monitor 1 (TE 42i-TL), the negative interference observed for NO_2 was the same magnitude as observed for the positive interference for NO, including the experiments with H_2O and CO (see Fig. 6 and Tables 2-3). This response is thought to arise as a consequence of the calculation methodology, combined with removal of alkenes during the NO_2 conversion by the Mo catalyst:

There are three modes of operation in monitor 1 (TE 42i-TL) – NO measurement, NO_2/NO_x measurement and background (pre-reactor) measurement, given by Eq 2-4 respectively:

$$s\mathrm{NO} = s\mathrm{NO}_{real} + X_i \quad \text{(Eq 2)}$$

$$s\mathrm{NOx} = s\mathrm{NOx}_{real} + yX_i \quad \text{(Eq 3)}$$

$$sP = fX_i \quad \text{(Eq 4)}$$

where sNO and sNOx are the NO and NO_x signals produced by the chemiluminescence monitor, respectively, $s\mathrm{NO}_{real}$ and $s\mathrm{NOx}_{real}$ are the 'real' NO and NO_x signals, X_i denotes the interference alkene *i*, *y* is the fraction of the interferant (alkene) X_i remaining after the Mo convertor, sP denotes signal at the pre-reactor and *f* is the fraction of X_i remaining after the pre-reactor. The mixing ratios of NO, NO_2 and NO_x are given by:

$$[\mathrm{NO}] = \frac{s\mathrm{NO} - sP}{c\mathrm{NO}} \quad \text{(Eq 5)}$$

$$[\mathrm{NO}] = \frac{(s\mathrm{NO}_{real} + X_i) - fX_i}{c\mathrm{NO}} \quad \text{(Eq 6)}$$

$$[\mathrm{NO}] = \frac{(s\mathrm{NO}_{real} + (1-f)X_i)}{c\mathrm{NO}} \quad \text{(Eq 7)}$$

$$[\mathrm{NOx}] = \frac{s\mathrm{NOx} - sP}{c\mathrm{NOx}} \quad \text{(Eq 8)}$$

$$[\mathrm{NOx}] = \frac{(s\mathrm{NOx}_{real} + yX_i) - fX_i}{c\mathrm{NOx}} \quad \text{(Eq 9)}$$

$$[\mathrm{NOx}] = \frac{(s\mathrm{NOx}_{real} + (y-f)X_i)}{c\mathrm{NOx}} \quad \text{(Eq 10)}$$

320

$$[\mathrm{NO_2}] = \frac{[\mathrm{NO_x}] - [\mathrm{NO}]}{CE} \quad \text{(Eq 11)}$$

$$[\mathrm{NO_2}] = \frac{(s\mathrm{NOx}_{real} + (y-f)X_i)}{c\mathrm{NOx} \times CE} - \frac{(s\mathrm{NO}_{real} + (1-f)X_i)}{c\mathrm{NO} \times CE} \quad \text{(Eq 12)}$$

where c is the 'span factor' and CE represents the conversion efficiency. If we assume cNOx ≈ cNO ≈ c, then

$$[\mathrm{NO_2}] = \frac{(s\mathrm{NOx}_{real} + (y-f)X_i) - (s\mathrm{NO}_{real} + (1-f)X_i)}{c \times CE} \quad \text{(Eq 13)}$$

325 From Eq 13, it may be seen that if $y = 1$ (*i.e.* if the interferant – alkene – abundance is not affected by passage through the Mo converter), then there would be no interference observed in the retrieved NO_2, while if the interferant species is subject to removal during passage through the converter, then $y < 1$ and a negative interference would be observed. Molybdenum oxide catalysts have been reported to efficiently isomerise alkenes at temperatures between 300 – 400 °C, (Wehrer *et al.*, 2003) and are also effective catalysts for the epoxidation of alkenes (Shen *et al.*, 2019). The observed small negative interference effects
330 (for monitors 1 and 2, the Mo converter units), in the absence of significant sampled NO_x, may reflect partial removal of the alkene on the converter.

The negative NO_2 interference apparent for monitors 3 and 4 (photolytic converter instruments) is more difficult to rationalise (as no Mo catalyst is present). Under ambient conditions, where NO_x is present, mechanism (3) may occur as outlined below.
335 In reality, the conversion efficiency for photolytic converters is substantially lower than 100% (Reed et al. 2016), as a consequence of both the finite photolysis intensity achievable, and occurrence of the NO + O_3 back reaction. If the instrument

calibration factor for NO_x is not equal to that for NO (see Eq 12), or if alkene was removed in the convertor stage, then this will lead to different interferences for NO and NO_2, as CE is also (significantly) less than 1. This trend is apparent in the values shown in Table 3, in particular for the instruments fitted with photolytic convertors. However, in the absence of sampled NO_x the observed less-positive or even negative NO_2 interference suggests that less alkene is present in the NO_x mode. Direct photolysis of alkenes is unlikely to cause such a change, considering the photolytic converter wavelength envelope, but photolytic production of HO_x radicals (which then react with the alkene) may be responsible.

Monitor 4 (AQD) used independent NO_2^* detection channels; tests were conducted using both channels for cis-2-butene and terpinolene systems, and revealed significant differences between the two detectors (*ca.* 40% lower interference response for NO in the NO_2 detection channel). With two independent detection channels, NO_2 may be determined from the NO_x measurement by either subtracting the NO level obtained from the NO channel (method (a)), or via the difference in signal observed in the NO_2/NO_x channel when turning the photolysis lamp on and off (method (b)). Under method (a), as employed for cis-2-butene and terpinolene, a lower positive interference from alkene chemiluminescence results, as a consequence of the difference in the detection cell conditions (results marked * in Table 3), while under method (b), as employed for the other alkenes studied here with the AQD system, the interference (from mechanism 4 alone) should cancel out (results marked # in Table 3).

Effect of quenching by the alkenes

The data presented in Figures 2-4 and Tables 2 and 3 show both negative and positive interferences while mechanism 4 alone would be expected to result in positive interference signals for NO for all alkenes. We therefore conclude that additional mechanisms are occurring. Under the conditions of these chamber experiments, retrieval of additional NO_y species can be precluded (the chamber wall source of HONO has been characterised and shown to produce ppt levels of HONO under the dark, dry conditions of these experiments (Zador *et al.*, 2005) and would be equally present for all experiments). We attribute the negative (or reduced positive) interference effects to a combination of mechanisms (1) and (3): quenching of excited OH (produced by alkene+ozone reaction) by alkenes – electron rich alkenes have been shown to be effective quenchers (Gersdorf *et al.*, 1987; Chang and Schuster, 1987) - and generation of HO_x radicals within the instrument following on from the ozonolysis reaction.

The alkene-ozone reactions are known to produce OH, HO_2 and RO_2 radicals both directly (e.g. Johnson and Marston, 2008), following the photolysis of other alkene-ozone reaction products (e.g. carbonyl compounds), and through OH-alkene reactions. Peroxy radicals promote the conversion of NO to NO_2, altering the abundance of both species (the formation of NO_x reservoirs such as nitric acid and organic nitrates will also occur, but will be negligible on the timescale of operation of most instruments).

The ozonolysis of TME results in the production of OH with close to unity yield (IUPAC, 2018) and if taking into account the above mechanism (4) only, might be expected to exhibit a large interference in NO mode. Table 2 shows no interference for monitors 1 and 2 (Mo convertor units) and negative and positive interferences for monitors 3 and 4 (photolytic convertor units) respectively, and so is hard to rationalise (for NO mode). The addition of CO as a scavenger for OH led to an increase in the NO signal for all monitors. A possible origin of this signal is the chemiluminescence production of the excited intermediate HOCO (from reaction of vibrationally excited OH, from the ozonolysis of TME, with CO), which has a temperature and pressure dependent rate of reaction, (Atkinson *et al.*, 2006; Li and Francisco, 2000) and is consistent with the larger NO signal in the photolytic monitors (Table 2).

Conclusion

The interference in chemiluminescence NO_x measurements from alkenes has been systematically investigated using four commercially available monitors. Varying degrees of interference in the NO and NO_2 signals were observed for all monitors investigated, attributed to a combination of mechanisms 1, 3 and 4, particularly the incomplete subtraction of chemiluminescence from the products of alkene-ozone reactions, manifest due to significant removal of the alkene during the instrument background cycle. Monoterpenes, α-terpinene and terpinolene, exhibit the largest interferences followed by 2,3-dimethyl-2-butene (TME) and trans-2-butene, in line with the calculated Kinetic Interference Potential, KIP (see Table 4). The KIP can be used as a crude indicator for a potential interference of an alkene to a NO signal, but have large margins of error as they do not take into account the variation in the yield of chemiluminescent products and other instrumental differences. The alkene interference observed with enhanced RH conditions also indicates the need to accurately calibrate chemiluminescence NO_x analysers under actual sampling conditions.

The NO interferences from alkenes among the monitors investigated in this study ranges from 1 to 11%. The varying responses exhibited by the different monitors reflect differences in the conditions within the instrument (ozone abundance, pressure and residence time) within the reaction cell and filter specifications. The magnitude of the NO and NO_2 interferences not only vary with different alkenes and commercial monitors, but will also be dependent upon sampling environments (and with ambient NO_x and alkenes concentrations). Notably, in these experiments the alkene abundance is high compared with most ambient air samples – consequently internally generated OH will react essentially exclusively with the alkene, which may not reflect ambient sampling – but which we do not expect to impact the conclusions reached with respect to mechanism 4, interference in retrieved NO levels. Further research to explore these impacts, and other parameters (*e.g.* H_2O abundance), is urgently needed. The chemiluminescence from monoterpene ozonolysis should also be investigated to identify emission spectra of possible interfering species; given the varying OH yields and energetics from the ozonolysis of different alkenes, their intensity of emission are likely to vary. A combination of selective long-pass filters and detector characteristics can then be exploited within chemiluminescence NO_x monitors to eliminate such interferences with similar emission spectra to NO_2*.

Mixing ratios of NO_x vary from > 100 ppb in some urban areas, *e.g.* Marylebone Road (Carslaw *et al.* 2005), < 300 ppt in biogenic environments (Hewitt *et al.* 2010) and < 35 ppt in remote areas (Lee et al. 2009). For typical urban environments where alkene mixing ratios are relatively low (< 2 ppb e.g. von Schneidemesser *et al.* 2010) the interferences identified here are not likely to be significant (~ 1% of the NO signal). However, for biogenic environments where monoterpenes and sesquiterpenes, which react rapidly with ozone, are abundant, the interference could be significantly larger. For example, average mixing ratios for isoprene (~ 1 ppb), 5 monoterpenes (~ 220 ppt), 3 short chain alkenes (~ 240 ppt) and NO (0.14 ppb) were measured within a south-east Asian tropical rainforest (Jones *et al.*, 2011). Using the relationship between KIP and NO interference an overestimation of NO levels of to up to 58% would result, with very significant implications for prediction of other atmospheric chemical processes involving NO_x. Given that NO_x mixing ratios are relatively small in biogenic and remote environments, these interferences could lead to their substantial overestimation. Such alkene interference may contribute to the relatively high NO and low NO_2 reported in the tropical rainforests at night, which could not otherwise be accounted for (Pugh *et al*. 2011).

Within indoor environments, NO_x primarily arises from outdoor sources or indoor combustion sources (Young *et al.*, 2019). Typically, in the absence of a known indoor combustion source, indoor NO levels are low (*ca.* 13% of outdoor levels) with NO_2 comprising the majority of the NO_x (Zhou *et al.*, 2019). There are multiple sources of alkenes indoors, such as fragranced volatile personal care products (Nemafollahi *et al.*, 2019; Yeoman *et al.*, 2020) and cleaning products (Kristenson *et al.*, 2019), resulting in very much larger levels than NO_x (McDonald *et al.*, 2018; Kristenson *et al.*, 2019). Consequently, monoterpenes are among the most ubiquitous VOC reported for indoor air, with the main species including, linalool, α-pinene, β-myrcene and limonene (Krol et al 2014; Nematollahi et al 2019). Peak limonene mixing ratios may be a factor of *ca*. 50 higher indoors than outdoor environments (Colman Lerner *et al.*, 2012). Although monoterpenes, α-pinene, myrcene and limonene show no significant NO interferences in chemiluminescence NO_x monitors, other fast reacting monoterpenes (with O_3) such as α-terpinene and terpinolene which are not generally reported in the literature, exhibit quite large interferences and may lead to very substantial overestimations in indoor NO_x measurements. Monoterpene mixing ratios in indoor environments can be further enhanced by cleaning activities (Singer *et al.*, 2006; Kristenson *et al.*, 2019; Weschler and Carslaw, 2018). Indoor α-terpinene and α-pinene mixing ratios have exceeded 10 and 68 ppb, respectively (Singer *et al.*, 2006; Brown *et al.*, 1994). These relatively large monoterpene mixing ratios may lead to substantial interferences in chemiluminescence NO_x monitors; their incorrect retrieval as measured "NO_x" will impact assessments of indoor air chemistry, indoor air quality and hence health.

Data Availability

Experimental data are available in the Eurochamp database, www.eurochamp.org, from the H2020 EUROCHAMP2020 project, GA no. 730997

Author Contributions

MSA, WJB and JDL conceived and planned the experiments. MSA, JDL, MV, AM and MR performed the experiments. LRC, LJK and MSA performed the data analysis. LRC, LJK, MSA, CF and WJB contributed to data investigation and curation. MSA wrote the original draft manuscript and all co-authors contributed to reviewing and editing the paper.

Competing Interests

The authors declare that they have no conflict of interest.

Acknowledgements

This work was funded in part through the UK Natural Environment Research Council (NERC) project "ICOZA: Integrated Chemistry of Ozone in the Atmosphere" (NE/ K012169/1) and by the EUROCHAMP-2 Transnational access project "NOxINT: NOx analyser interference in chemically complex mixtures" (E2-2010-05-26-0033) . Part of this work has received funding from the European Union's Horizon 2020 research and innovation programme through the EUROCHAMP-2020 Infrastructure Activity under grant agreement No. 730997. CEAM is partly supported by the IMAGINA-Prometeo project (PROMETEO2019/110) and by Generalitat Valenciana. In addition, we thank Eva Clemente for their work in these experiments.

References

Alam, M. S., Camredon, M., Rickard, A. R., Carr, T., Wyche, K. P., Hornsby, K. E., Monks, P. S., and Bloss, W. J.: Total radical yields from tropospheric ethene ozonolysis, Phys Chem Chem Phys, 13, 11002-11015, 2011.

Alam, M. S., Rickard, A. R., Camredon, M., Wyche, K. P., Carr, T., Hornsby, K. E., Monks, P. S., and Bloss, W. J.: Radical product yields from the ozonolysis of short chain alkenes under atmospheric boundary layer conditions, J Phys Chem A, 117, 12468-12483, 2013.

Atkinson, R., Baulch, D.L., Cox, R.A., Crowley, J.N., Hampson, R.F., Hynes, R.G., Jenkin, M.E., Rossi, M.J. and Troe, J.: Evaluated kinetic and photochemical data for atmospheric chemistry: Volume II – gas phase reactions of organic species, Atmos. Chem. Phys., 6, 3625-4055, 2006.

AQEG: Air quality expert group. Nitrogen dioxide in the United Kingdom, 2004.

Brown, S.K., Sim, M.R., Abramson, M.J. and Gray, C.N.: Concentrations of volatile organic compounds in indoor air–a review, Indoor air, 4, 2, 123-134, 1994

BS EN 14211: Ambient air. Standard method for the measurement of the concentration of nitrogen dioxide and nitrogen monoxide by chemiluminescence, The British Standards Institution, 2012

Cape, J. N.: The Use of Passive Diffusion Tubes for Measuring Concentrations of Nitrogen Dioxide in Air, Critical Reviews in Analytical Chemistry, 39, 289-310, 2009.

Carslaw, D. C.: Evidence of an increasing NO2/NOX emissions ratio from road traffic emissions, Atmospheric Environment, 39, 4793-4802, 2005.

Carslaw, D. C. and Rhys-Tyler, G.: New insights from comprehensive on-road measurements of NOx, NO2 and NH3 from vehicle emission remote sensing in London, UK, Atmospheric Environment, 81, 339-347, 2013.

Chaloulakou, A., Mavroidis, I., and Gavriil, I.: Compliance with the annual NO2 air quality standard in Athens. Required NOx levels and expected health implications, Atmospheric Environment, 42, 454-465, 2008.

Chang, S. L. P. and Schuster, D. I.: Fluorescence quenching of 9,10-dicyanoanthracene by dienes and alkenes, The Journal of Physical Chemistry, 91, 3644-3649, 1987.

Crawford, J., Davis, D., Chen, G., Bradshaw, J., Sandholm, S., Kondo, Y., Merrill, J., Liu, S., Browell, E., and Gregory, G.: Implications of large scale shifts in tropospheric NO x levels in the remote tropical Pacific, Journal of Geophysical Research: Atmospheres, 102, 28447-28468, 1997.

Dillon, T. J. and Crowley, J. N.: Reactive quenching of electronically excited NO2∗ and NO3∗ by H2O as potential sources of atmospheric HOx radicals, Atmos. Chem. Phys., 18, 14005-14015, 2018.

Dunlea, E. J., Herndon, S. C., Nelson, D. D., Volkamer, R. M., San Martini, F., Sheehy, P. M., Zahniser, M. S., Shorter, J. H., Wormhoudt, J. C., Lamb, B. K., Allwine, E. J., Gaffney, J. S., Marley, N. A., Grutter, M., Marquez, C., Blanco, S., Cardenas, B., Retama, A., Ramos Villegas, C. R., Kolb, C. E., Molina, L. T., and Molina, M. J.: Evaluation of nitrogen dioxide chemiluminescence monitors in a polluted urban environment, Atmos. Chem. Phys., 7, 2691-2704, 2007.

495

European Environmental Agency.: Air quality in Europe - 2018 report, ISSN 1997-8449, Report No: TH-AL-18-013-EN-N, 2018.

Finlayson, B., Pitts Jr, J., and Atkinson, R.: Low-pressure gas-phase ozone-olefin reactions. Chemiluminescence, kinetics, and
500 mechanisms, Journal of the American Chemical Society, 96, 5356-5367, 1974.

Fuchs, H., Dubé, W. P., Lerner, B. M., Wagner, N. L., Williams, E. J., and Brown, S. S.: A sensitive and versatile detector for atmospheric NO2 and NOx based on blue diode laser cavity ring-down spectroscopy, Environmental science & technology, 43, 7831-7836, 2009.

505

Gerboles, M., Lagler, F., Rembges, D., and Brun, C.: Assessment of uncertainty of NO2 measurements by the chemiluminescence method and discussion of the quality objective of the NO2 European Directive, Journal of Environmental Monitoring, 5, 529-540, 2003.

510 Gersdorf, J., Mattay, J., and Goerner, H.: Photoreactions of biacetyl, benzophenone, and benzil with electron-rich alkenes, J. Am. Chem. Soc.; (United States), 1987. Medium: X; Size: Pages: 1203-1209, 1987.

Goldstein, A. H. and Galbally, I. E.: Known and Unexplored organic constituents in the Earth's Atmosphere, Environmental Science and Technology, 2007. 1515-1521, 2007.

515

Grice, S., Stedman, J., Kent, A., Hobson, M., Norris, J., Abbott, J., and Cooke, S.: Recent trends and projections of primary NO2 emissions in Europe, Atmospheric Environment, 43, 2154-2167, 2009.

Hansen, D., Atkinson, R., and Pitts Jr, J.: Structural effects on the chemiluminescence from the reaction of ozone with selected
520 organic compounds, Journal of Photochemistry, 7, 379-404, 1977.

Heard, D.: Analytical techniques for atmospheric measurement, John Wiley & Sons, 2008.

Hewitt, C. N., Lee, J. D., MacKenzie, A. R., Barkley, M. P., Carslaw, N., Carver, G. D., Chappell, N. A., Coe, H., Collier, C., Commane, R., Davies, F., Davison, B., DiCarlo, P., Di Marco, C. F., Dorsey, J. R., Edwards, P. M., Evans, M. J., Fowler, D., Furneaux, K. L., Gallagher, M., Guenther, A., Heard, D. E., Helfter, C., Hopkins, J., Ingham, T., Irwin, M., Jones, C., Karunaharan, A., Langford, B., Lewis, A. C., Lim, S. F., MacDonald, S. M., Mahajan, A. S., Malpass, S., McFiggans, G., Mills, G., Misztal, P., Moller, S., Monks, P. S., Nemitz, E., Nicolas-Perea, V., Oetjen, H., Oram, D. E., Palmer, P. I., Phillips, G. J., Pike, R., Plane, J. M. C., Pugh, T., Pyle, J. A., Reeves, C. E., Robinson, N. H., Stewart, D., Stone, D., Whalley, L. K., and Yin, X.: Overview: oxidant and particle photochemical processes above a south-east Asian tropical rainforest (the OP3 project): introduction, rationale, location characteristics and tools, Atmos. Chem. Phys., 10, 169-199, 2010.

Hills, A. J. and Zimmerman, P. R.: Isoprene measurement by ozone-induced chemiluminescence, Analytical Chemistry, 62, 1055-1060, 1990.

Jernigan, J.R.: Chemiluminescence NOx and GFC NDIR CO analyzers for low level source monitoring. *Thermo Environmental Instruments, USA,* 2001.

Johnson, D. and Marston, G.: The gas-phase ozonolysis of unsaturated volatile organic compounds in the troposphere, Chem Soc Rev, 37, 699-716, 2008.

Jones, C.E., Hopkins, J.R. and Lewis, A.C.: In situ measurements of isoprene and monoterpenes within a south-east Asian tropical rainforest, Atmospheric chemistry and Physics, 11, 14, 6971, 2011

Kasyutich, V.L., Bale, C.S.E., Canosa-Mas, C.E., Pfrang, C., Vaughan, S. and Wayne, R.P.: Cavity-enhanced absorption: detection of nitrogen dioxide and iodine monoxide using a violet laser diode, Applied Physics B, 76, 691-697, 2003.

Kebabian, P. L., Herndon, S. C., and Freedman, A.: Detection of Nitrogen Dioxide by Cavity Attenuated Phase Shift Spectroscopy, Analytical Chemistry, 77, 724-728, 2005.

Keuken, M., Roemer, M., and van den Elshout, S.: Trend analysis of urban NO2 concentrations and the importance of direct NO2 emissions versus ozone/NOx equilibrium, Atmospheric Environment, 43, 4780-4783, 2009.

Kristensen, K., Lunderberg, D. M., Liu, Y., Misztal, P.K., Tian, Y., Arata, C., Nazaroff, W. W. and Goldstein, A.H.: Sources and dynamics of semivolatile organic compounds in a single-family residence in northern California. Indoor Air, 29, 4, 645-655, 2019.

Król, S., Namieśnik, J. and Zabiegała, B.: α-Pinene, 3-carene and d-limonene in indoor air of Polish apartments: The impact on air quality and human exposure. Science of the total environment, 468, 985-995, 2014.

Lamsal, L., Martin, R., Van Donkelaar, A., Steinbacher, M., Celarier, E., Bucsela, E., Dunlea, E., and Pinto, J.: Ground-level nitrogen dioxide concentrations inferred from the satellite-borne Ozone Monitoring Instrument, Journal of Geophysical Research: Atmospheres, 113, 2008.

Lee, J. D., Moller, S. J., Read, K. A., Lewis, A. C., Mendes, L., and Carpenter, L. J.: Year-round measurements of nitrogen oxides and ozone in the tropical North Atlantic marine boundary layer, Journal of Geophysical Research: Atmospheres, 114, 2009.

Lerner, J.C., Sanchez, E.Y., Sambeth, J.E. and Porta, A.A.: Characterization and health risk assessment of VOCs in occupational environments in Buenos Aires, Argentina, Atmospheric environment, 55, 440-447, 2012.

Li, Y. and Francisco, J.S.: High level ab initio studies on the excited states of HOCO radical. The Journal of Chemical Physics, 113, 18, 7963-7970, 2000

Matthews, R. D., Sawyer, R. F., and Schefer, R. W.: Interferences in chemiluminescent measurement of nitric oxide and nitrogen dioxide emissions from combustion systems, Environmental Science & Technology, 11, 1092-1096, 1977.

McDonald, B.C., de Gouw, J.A., Gilman, J.B., Jathar, S.H., Akherati, A., Cappa, C.D., Jimenez, J.L., Lee-Taylor, J., Hayes, P.L., McKeen, S.A. and Cui, Y.Y.: Volatile chemical products emerging as largest petrochemical source of urban organic emissions, Science, 359, 6377, 760-764, 2018.

Muñoz, A., Vera, T., Sidebottom, H., Mellouki, A., Borrás, E., Ródenas, M., Clemente, E., and Vázquez, M.: Studies on the Atmospheric Degradation of Chlorpyrifos-Methyl, Environmental Science & Technology, 45, 1880-1886, 2011.

Murphy, J. G., Day, D. A., Cleary, P. A., Wooldridge, P. J., Millet, D. B., Goldstein, A. H., and Cohen, R. C.: The weekend effect within and downwind of Sacramento – Part 1: Observations of ozone, nitrogen oxides, and VOC reactivity, Atmos. Chem. Phys., 7, 5327-5339, 2007.

Navas, M. J., Jiménez, A. M., and Galán, G.: Air analysis: determination of nitrogen compounds by chemiluminescence, Atmospheric Environment, 31, 3603-3608, 1997.

Nematollahi, N., Kolev, S. D. and Steinemann, A.: Volatile chemical emissions from 134 common consumer products. Air Quality, Atmosphere & Health, 12, 11, 1259-1265, 2019.

Pitts Jr, J.N., Kummer, W.A., Steer, R.P., and Finlayson, B.J.: The chemiluminescent reactions of ozone with olefins and organic sulphides, Advances in Chemistry, 113, 10, 246-254, 1972.

Pugh, T. A. M., Ryder, J., MacKenzie, A. R., Moller, S. J., Lee, J. D., Helfter, C., Nemitz, E., Lowe, D., and Hewitt, C. N.: Modelling chemistry in the nocturnal boundary layer above tropical rainforest and a generalised effective nocturnal ozone deposition velocity for sub-ppbv NOx conditions, Journal of Atmospheric Chemistry, 65, 89-110, 2010.

Reed, C., Evans, M. J., Di Carlo, P., Lee, J. D., and Carpenter, L. J.: Interferences in photolytic NO2 measurements: explanation for an apparent missing oxidant?, Atmos. Chem. Phys., 16, 4707-4724, 2016.

Sandholm, S., Bradshaw, J., Dorris, K., Rodgers, M., and Davis, D.: An airborne compatible photofragmentation two-photon laser-induced fluorescence instrument for measuring background tropospheric levels of NO, NO x, and NO2, Journal of Geophysical Research: Atmospheres, 95, 10155-10161, 1990.

Schurath, U., Guesten, H., and Penzhorn, R.-D.: Phosphorescence of α-diketones from ozone-olefin reactions, Journal of Photochemistry, 5, 33-40, 1976.

Shen, Y., Jiang, P., Wai, P. T., Gu, Q., and Zhang, W.: Recent Progress in Application of Molybdenum-Based Catalysts for Epoxidation of Alkenes, Catalysts, 9, 31, 2019.

Shrivastava, M., Cappa, C. D., Fan, J., Goldstein, A. H., Guenther, A. B., Jimenez, J. L., Kuang, C., Laskin, A., Martin, S. T., and Ng, N. L.: Recent advances in understanding secondary organic aerosol: Implications for global climate forcing, Reviews of Geophysics, 55, 509-559, 2017.

Singer, B.C., Coleman, B.K., Destaillats, H., Hodgson, A.T., Lunden, M.M., Weschler, C.J. and Nazaroff, W.W.: Indoor secondary pollutants from cleaning product and air freshener use in the presence of ozone, Atmospheric Environment, 40, 35, 6696-6710, 2006.

Steinbacher, M., Zellweger, C., Schwarzenbach, B., Bugmann, S., Buchmann, B., Ordonez, C., Prévôt, A. S., and Hueglin, C.: Nitrogen oxide measurements at rural sites in Switzerland: Bias of conventional measurement techniques, Journal of Geophysical Research: Atmospheres, 112, 2007.

Thalman, R., and Volkamer, R.: Inherent calibration of a blue LED-CE-DOAS instrument to measure iodine oxide, glyoxal, methyl glyoxal, nitrogen dioxide, water vapour and aerosol extinction in open cavity mode. Atmos. Meas. Tech., 3, 1797-1814, 2010.

Toby, S.: Chemiluminescence in the reactions of ozone, Chemical Reviews, 84, 277-285, 1984.

USEPA: Quality assurance handbook. Reference method for determination of nitrogen dioxide in the atmosphere (chemiluminescence), 2.3, 2, 2002.

Velasco, E., Lamb, B., Westberg, H., Allwine, E., Sosa, G., Arriaga-Colina, J. L., Jobson, B. T., Alexander, M. L., Prazeller, P., Knighton, W. B., Rogers, T. M., Grutter, M., Herndon, S. C., Kolb, C. E., Zavala, M., de Foy, B., Volkamer, R., Molina, L. T., and Molina, M. J.: Distribution, magnitudes, reactivities, ratios and diurnal patterns of volatile organic compounds in the Valley of Mexico during the MCMA 2002 & 2003 field campaigns, Atmos. Chem. Phys., 7, 329-353, 2007.

Villena, G., Bejan, I., Kurtenbach, R., Wiesen, P., and Kleffmann, J.: Development of a new Long Path Absorption Photometer (LOPAP) instrument for the sensitive detection of NO_2 in the atmosphere, Atmospheric Measurement Techniques Discussions, 4, 1751-1793, 2011.

Villena, G., Bejan, I., Kurtenbach, R., Wiesen, P., and Kleffmann, J.: Interferences of commercial NO_2 instruments in the urban atmosphere and in a smog chamber, Atmos. Meas. Tech., 5, 149-159, 2012.

von Schneidemesser, E., Monks, P. S., and Plass-Duelmer, C.: Global comparison of VOC and CO observations in urban areas, Atmospheric Environment, 44, 5053-5064, 2010.

Wehrer, P., Libs, S., and Hilaire, L.: Isomerization of alkanes and alkenes on molybdenum oxides, Applied Catalysis A: General, 238, 69-84, 2003.

Weschler, C.J. and Carslaw, N.: Indoor chemistry, Environ. Sci. Technol, 52, 2419−2428, 2018.

Wiesen, P.: Photooxidant Studies Using the European Photoreactor EUPHORE, Berlin, Heidelberg, 2001, 155-162.

Yeoman, A. M., Shaw, M., Carslaw, N., Murrells, T., Passant, N., Lewis, A. C.: Simplified speciation and atmospheric volatile organic compounds emission rates from non-aerosol personal care products. Indoor Air. 0, 1– 14, 2020

Young, C.J., Zhou, S., Siegel, J.A. and Kahan, T.F.: Illuminating the dark side of indoor oxidants. Environmental Science: Processes & Impacts, 21, 8, 1229-1239, 2019.

Zhou, S., Young, C. J., VandenBoer, T. C. and Kahan, T. F.: Role of location, season, occupant activity, and chemistry in indoor ozone and nitrogen oxide mixing ratios. Environmental Science: Processes & Impacts, 21, 8, 1374-1383, 2019.

Table 1: Details of the NO_x monitoring instruments used.

Number	Manufacturer	Model	Institution	NO_2 Convertor	Limit of Detection (LOD)*	
					NO (ppt)	NO_2 (ppt)
1	Thermo	TE42i-TL	Birmingham	Heated Mo	210	210
2	API	200AU	EUPHORE	Heated Mo	190	450
3	Eco Physics	CLD 770 Alppt / PLC 760	EUPHORE	Xe lamp	150	430
4	Air Quality Designs	-	York	Blue light at 395 nm	60	150

*Calculated in this study

720

Table 2: Measured NO interference (% ± 1 s.d. of the slope) for each monitor across a range of different alkenes (LOD: Limit of Detection).

Species	*1: TE 42i-TL*	*2: API 200AU*	*3: Eco Physics CLD770*	*4: Air Quality Designs*
cis-2-butene	< LOD	< LOD	0.40 ± 0.05	0.38 ± 0.01
TME	< LOD	< LOD	-0.70 ± 0.09	1.10 ± 0.01
Trans-2-butene	< LOD	< LOD	1.00 ± 0.01	0.83 ± 0.01
Terpinolene	0.50 ± 0.05	< LOD	1.30 ± 0.01	4.40 ± 0.15
α-Terpinene	1.90 ± 0.05	0.50 ± 0.04	2.30 ± 0.04	10.9 ± 0.06
Limonene	< LOD	< LOD	< LOD	-0.10 ± 0.01
TME + H_2O	< LOD	< LOD	0.60	2.40
Trans-2-butene + H_2O	< LOD	< LOD	0.48 ± 0.01	0.37±0.01
Terpinolene + H_2O	0.25 ± 0.03	< LOD	0.88 ± 0.01	1.60 ± 0.10
α-Terpinene + H_2O	1.00 ± 0.07	< LOD	1.30 ± 0.06	6.20 ± 0.70
TME + CO	0.70 ± 0.01	0.66 ± 0.09	1.30 ± 0.12	1.40 ± 0.02

730

735

740

745

Table 3: Measured NO_2 interference (% ± 1 s.d. of the slope) for each monitor across a range of different alkenes (LOD: Limit of Detection).

Species	*1: TE 42i-TL*	*2: API 200AU*	*3: Eco Physics CLD770*	*4: Air Quality Designs*
cis-2-butene	-0.60 ± 0.10	< LOD	-1.10 ± 0.08	0.30 ± 0.02*
TME	-0.63 ± 0.05	< LOD	-0.78 ± 0.15	-0.92 ± 0.10#
Trans-2-butene	-0.50 ± 0.06	< LOD	-0.50 ± 0.03	-0.93 ± 0.02#
Terpinolene	-0.61 ± 0.02	< LOD	-0.18 ± 0.03	1.60 ± 0.10*
α-Terpinene	-1.90 ± 0.13	< LOD	-1.00. ± 0.20	3.10 ± 2.10
Limonene	< LOD	< LOD	< LOD	0.09 ± 0.01#
TME + H_2O	-0.60	< LOD	< LOD	-2.00
Trans-2-butene + H_2O	< LOD	< LOD	< LOD	-0.41 ±0.02
Terpinolene + H_2O	-0.29 ± 0.02	< LOD	< LOD	-0.25
α-Terpinene + H_2O	-0.98 ± 0.06	< LOD	< LOD	0.35±0.10
TME + CO	-0.70±0.01	< LOD	< LOD	1.00 ± 0.30

775

Table 4: Kinetic ranking of interference potential: the percentage of the potential chemiluminescent signal from ozonolysis of a given alkene which would not be removed by a standard instrument background cycle, under conditions (ozone mixing ratio, residence time) which would remove 99% of the NO sampled. Rate constants are taken from Calvert et al. (2000); $k_{(NO+O3)}$= 1.90 × 10^{-14} cm^3 $molecule^{-1}$ s^{-1} (298 K). NB: this ranking does not include variations in the yield of chemiluminescent products with alkene structure, which will modulate the values given. Species marked * are investigated in this study.

780

Species	$k_{(Alkene+O3)}$ (298 K) /cm^3 $molecule^{-1}$ s^{-1}	Kinetic Interference Potential (%)	No. of C=C bonds	No. of terminal C=C bonds
Ethene	1.58×10^{-18}	0.04 *	1	1
1-Butene	9.64×10^{-18}	0.23	1	1
2,3-dimethyl-1-butene	1.00×10^{-17}	0.24	1	1
Propene	1.01×10^{-17}	0.24 *	1	1
1-pentene	1.06×10^{-17}	0.26	1	1
Isobutene	1.13×10^{-17}	0.27 *	1	1
Isoprene	1.28×10^{-17}	0.31 *	1	1
2-methyl-1-butene	1.30×10^{-17}	0.31	1	1
β-pinene	1.50×10^{-17}	0.36 *	1	1
α-cedrene	2.80×10^{-17}	0.68	1	0
3-carene	3.70×10^{-17}	0.89	1	0
α-pinene	8.66×10^{-17}	2.08 *	1	0
cis-2-butene	1.25×10^{-16}	2.98 *	1	0
cis-3-hexane	1.44×10^{-16}	3.43	1	0
trans-3-hexane	1.57×10^{-16}	3.73	1	0
α-coapene	1.58×10^{-16}	3.76	1	0
trans-2-butene	1.90×10^{-16}	4.50 *	1	0
Limonene	2.00×10^{-16}	4.73 *	2	1
2-carene	2.30×10^{-16}	5.42	1	0
2-methyl-2-butene	4.03×10^{-16}	9.31	1	0
Myrcene	4.70×10^{-16}	10.77 *	3	2
2,3-dimethyl-2-butene	1.13×10^{-15}	23.96 *	1	0
Terpinolene	1.90×10^{-15}	36.90 *	2	0
α-humulene	1.20×10^{-14}	94.54	3	0
β-carophyllene	1.20×10^{-14}	94.54	2	1
α-terpinene	2.10×10^{-14}	99.38 *	2	0

785

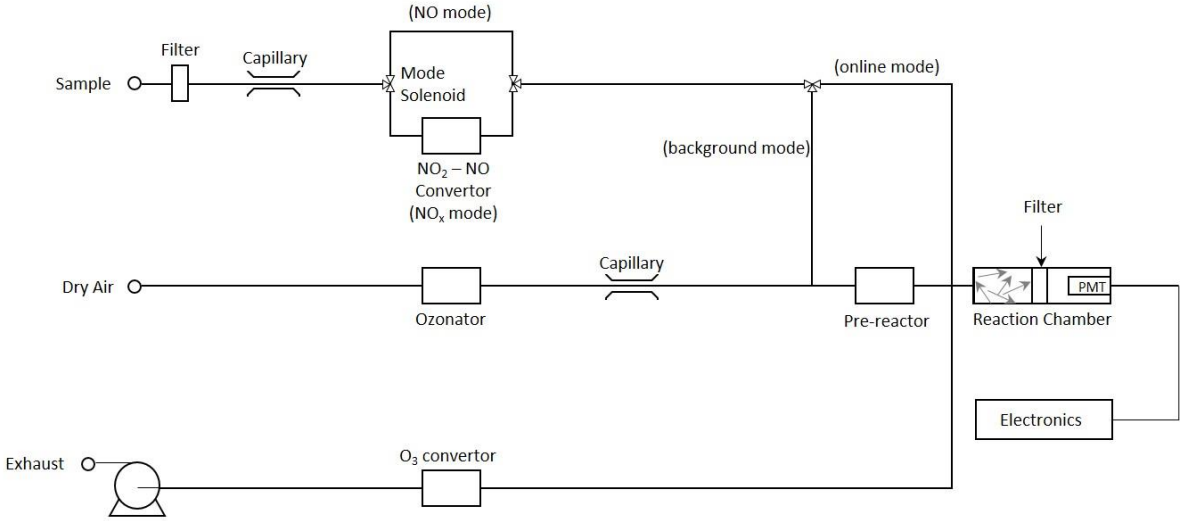

Figure 1: A typical flow schematic of a chemiluminescent NO monitor.

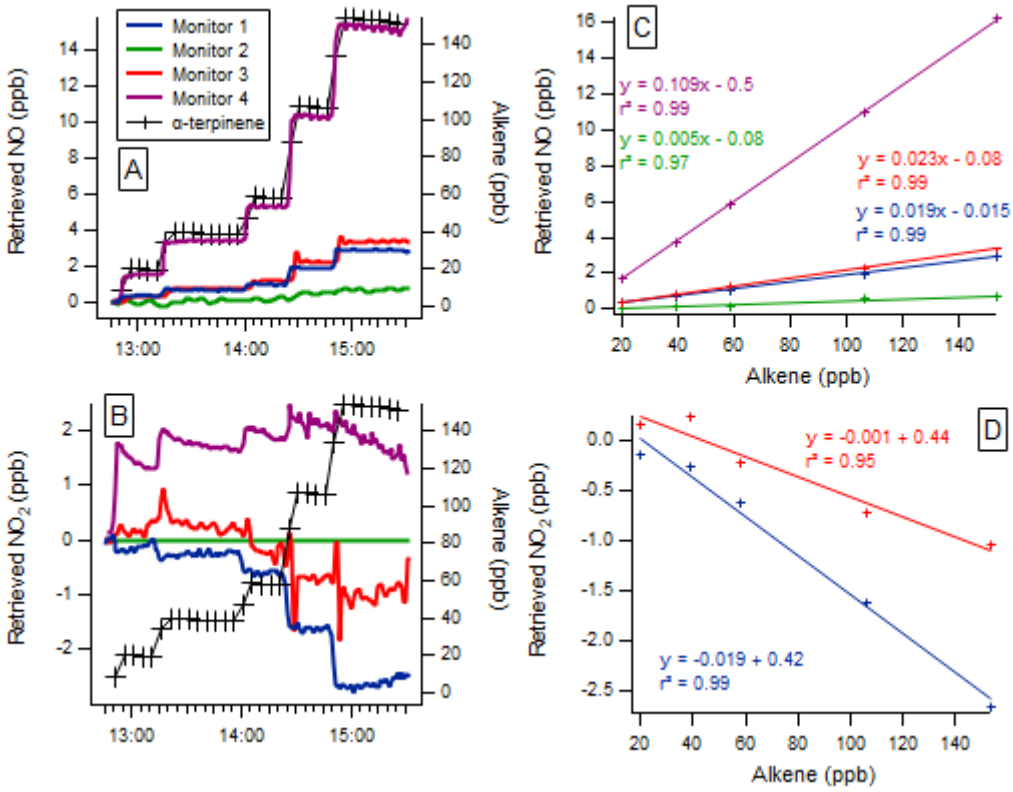

Figure 2: Time series of the α-terpinene mixing ratio and indicated / "measured" NO (top) and NO_2 (bottom) mixing ratios as directly retrieved by each monitor (left column) with 1 minute time resolution and the regression calculations for the monitors that demonstrated significant interference with the addition of α-terpinene (right column). Note the different y-axis scales.

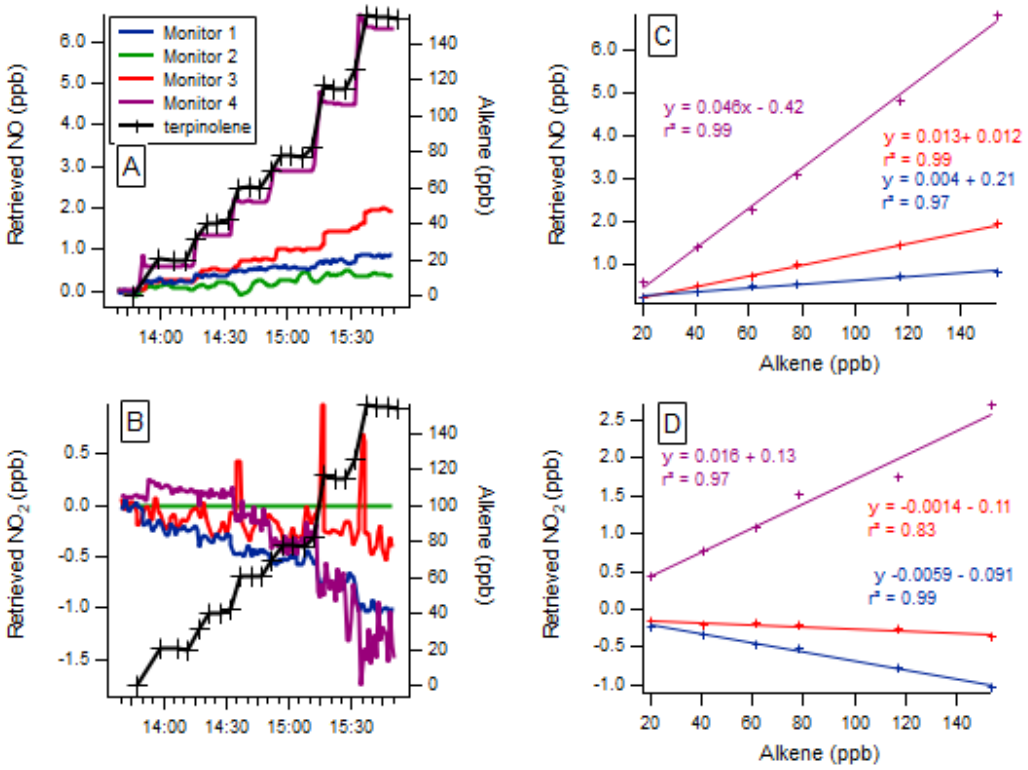

Figure 3: Time series of the terpinolene mixing ratio and measured NO and NO_2 mixing ratios as retrieved by each monitor (left column) with 1 minute time resolution and the regression calculations for the monitors that demonstrated significant interference with the addition of terpinolene (right column). Note the different y-axis scales.

830

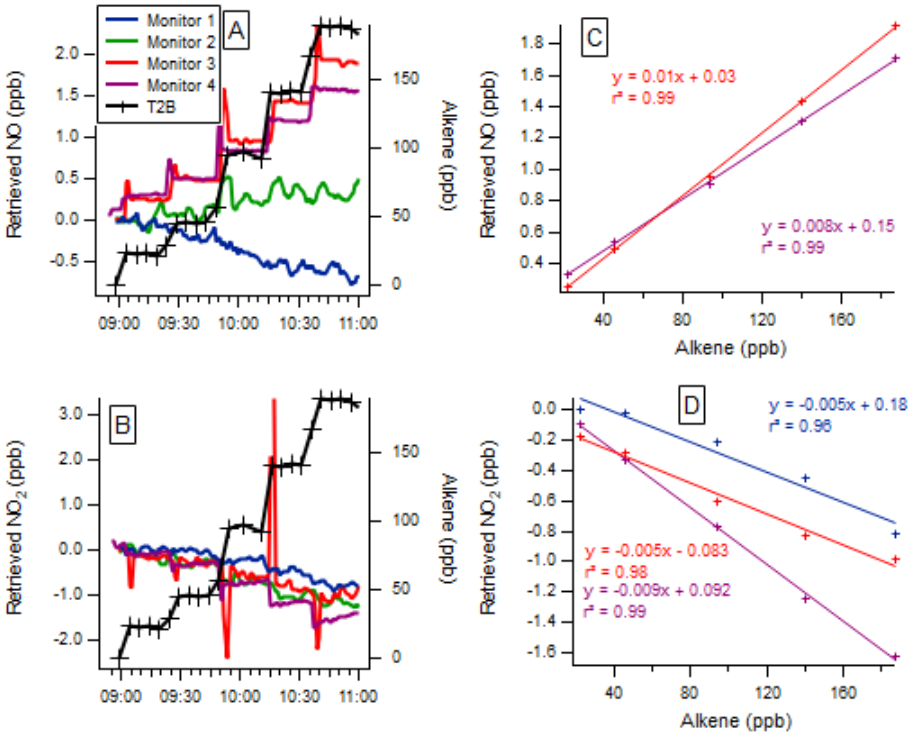

Figure 4: Time series of the trans-2-butene (T2B) mixing ratio and measured NO (top) and NO_2 (bottom) mixing ratios as retrieved by each monitor (left column) with 1 minute time resolution and the regression calculations for the monitors that demonstrated significant interference with the addition of T2B (right column). Note the different y-axis scales.

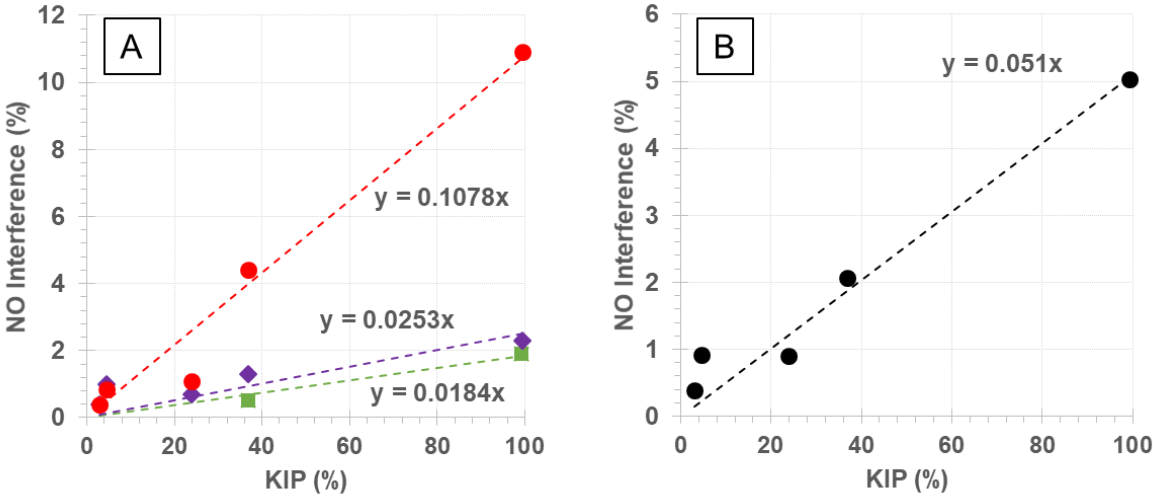

Figure 5: Relationship between measured NO interference (%) and kinetic interference potential, KIP (%) for monitors 1 (green), 3 (purple), 4 (red) and the average of the observed NO interference across all instruments (black).

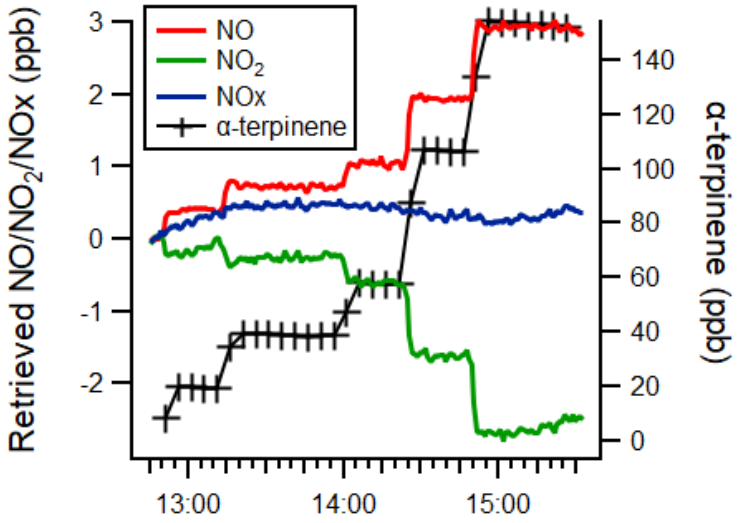

Figure 6: Time series of the α-terpinene mixing ratio (black) and measured NO (red), NO_2 (green) and NO_x (blue) mixing ratios as retrieved by monitor 1 (TE 42i-TL) with 1 minute time resolution.